

FOREWORD

The work reported here was performed by Atomics International, a Division of North American Aviation, Inc., under the auspices of the Department of Defense through the Advanced Research Project Agency. Contract AF 33(616)-6794, issued under ARPA Order No. 24-60, Project 4776, "Materials Thermal Properties," was administered by the Directorate of Materials and Processes, Deputy for Technology, Aeronautical Systems Div., with Mr. Hyman Marcus acting as project engineer. This report covers work conducted from August 1, 1960 to July 31, 1961.

At the beginning of the period covered by this report, this work was performed within the Solid State Ceramics Group headed by Dr. J. E. Hove. The Solid State Ceramics Group has been dissolved and Dr. Hove has left our organization. This investigation is now being carried out within the Thermoelectric and High Temperature Materials Section under the responsible supervision of Dr. N. R. Mukherjee, Section Leader.

The project is indebted to Mr. R. S. Carpenter for able technical assistance in the construction of the transient measurements apparatus, and to Mr. R. A. Finch for his assistance in the development of the pulse-heating apparatus.

Contrails

ABSTRACT

Refinements in the transient thermal property apparatus are described. With these modifications, the apparatus has been used to determine the thermal diffusivity of tungsten boride from about 1300°C to 1600°C. The measured values increase from about 0.054 to 0.058 over this temperature interval.

The techniques and apparatus for measuring the specific heat of brittle conductors by pulse heating are also described. Resistivity and specific heat data for uranium silicide of several compositions are reported. The resistivity and specific heat increased with increasing silicon content. For uranium silicide containing 3.8% silicon, the resistivity increased from 56 micro-ohm-cm at 0°C to 75 micro-ohm-cm at 750°C and for uranium silicide containing 5.9% silicon, the resistivity increased from 81 micro-ohm-cm at 0°C to 111 micro-ohm-cm at 800°C. The specific heat for the 3.8% silicon material is given by $c_p = 3.16 \times 10^{-6}T + 0.0412$ cal/gm-°C from 50° to 430°C, and for the 5.8% silicon material, $c_p = 16.1 \times 10^{-6}T + 0.0455$ cal/gm-°C from 50° to 715°C, where T is in °C.

The thermal conductivity of titanium carbide was measured over the temperature region 400° to 1200°C. The steady-state radial heat flow method was used. The conductivity varies linearly from 0.088 cal/sec-cm-°C at 500°C to 0.109 cal/sec-cm-°C at 1100°C. These results are in marked contrast to values reported in the literature.

This report has been reviewed and approved.



JULES I. WITTEBORT
Chief, Thermophysics Branch
Physics Laboratory
Directorate of Materials and Processes

TABLE OF CONTENTS

	Page
I. INTRODUCTION	1
II. STATUS REPORT ON TRANSIENT THERMAL PROPERTY MEASUREMENTS	2
III. SPECIFIC HEAT OF BRITTLE CONDUCTORS BY THE PULSE HEATING METHOD.	10
IV. THERMAL CONDUCTIVITY BY STEADY-STATE METHOD	17
V. BIBLIOGRAPHY	22

LIST OF FIGURES

Figure		Page
1.	Transient Measurements Apparatus	3
2.	Schematic of Radiation Shields With Pyrometer Sight Tubes.	5
3.	Thermal Response Curves for Tungsten Boride Sample	7
4.	Time Rate of Heat Input to Tungsten Boride Sample	7
5.	Specific Heat Apparatus	10
6.	Closeup of Mounted Sample	13
7.	Electrically Machined Specimens for Specific Heat Measurements	13
8.	Resistivity of Uranium Silicide	14
9.	Specific Heat Capacity of Uranium Silicide	15
10.	Steady-State Thermal Conductivity Furnace	18
11.	Thermal Conductivity of Titanium Carbide	19
12.	Electrical Resistivity of Titanium Carbide	19
13.	Electrical Resistivity of Zirconium Carbide	21

LIST OF TABLES

Table Number		Page
1.	Thermal Diffusivity of Tungsten Boride	8
2.	Sample Histories of Uranium Silicide	12
3.	Calculated Specific Heats of Uranium Silicides	16

THERMAL PROPERTIES OF REFRACTORY MATERIALS

by J. A. Cape and R. E. Taylor

I. INTRODUCTION

The objective of this research program is to measure and describe the high-temperature behavior of thermal properties of refractory materials for rocket nozzle applications. Representative materials of interest are the carbides, borides, and nitrides of tantalum, tungsten, etc.

Recent development in the program for measuring thermal diffusivity and specific heat by analysis of the transient thermal response of the sample are reported in Section I of this report. Some recent measurements on tungsten boride by the transient method are presented and discussed.

Section II of this report deals with the development of the pulse heating specific heat apparatus and its application to brittle conductors. Some measurements on titanium and zirconium carbide are presented.

In Section III the thermal conductivity of titanium carbide as measured by a steady-state apparatus is reported. Results are compared with previous data in the literature.

Manuscript released by the author July, 1961 for publication as a WADD technical report.

WADD TR 60-581, Pt 2

1

II. STATUS REPORT ON TRANSIENT THERMAL PROPERTY MEASUREMENTS

An apparatus for the measurement of the thermal properties of samples under transient heating conditions has been under construction and development during this reporting period. In this scheme, the sample is entirely enclosed, *in vacuo*, within a heater and radiation shields. This configuration permits eliminating heat losses through conduction, radiation, or convection which might not otherwise be accounted for. The details of this approach have been reported previously.¹ Power is supplied to the heater by inductive coupling to the radio-frequency coil of a 389.6 kc/sec Lepel Induction Furnace of 5 kw output. The heater, concentrator, and primary coil are entirely enclosed within the cylindrical pyrex vacuum enclosure which is shown in the center of Figure 1. This permits placing the heater concentrator and coil as close together as possible so as to optimize coupling.

A general description of the apparatus was given previously.¹ The present arrangement, however, differs somewhat from that previously described. Inasmuch as the pyrometer optics, the recording electronics, and the radiation shield geometry have proved to be critical from the point of view of temperature measurement, it is pertinent to describe the present arrangement and the considerations which prescribed the modifications.

A quantitative estimate of what is required by way of temperature measurement in the transient scheme may be deduced by considering the equations from which the thermal diffusivity and specific heat are determined.

The thermal diffusivity is given approximately by:¹

$$\alpha = \frac{a^2}{8\Delta t} \quad (1)$$

when a is the radius of the sample and Δt is the time separating two points at the same temperature on the temperature-time curves of the two holes in the sample, one at the center (cf Figure 6 of reference 1), and the other at $r = a/\sqrt{2}$. For example, for a typical carbide, when $\alpha \approx 0.05 \text{ cm}^2/\text{sec}$, $\Delta t \approx 1 \text{ sec}$ or less. Consequently, on a scale where a temperature change of several hundred degrees is recorded in a time of the order of minutes, and where the temperature derivative is of the order of $1 \text{ }^\circ\text{C}/\text{sec}$, the pyrometer must be sensitive to and record accurately temperature differences of much less than $1 \text{ }^\circ\text{C}$ for accuracy in thermal diffusivity measurements. In practice this means one must measure the time separating two curves which are less than one second apart, and have very shallow slopes. This places severe requirements on the noise level of the temperature-measuring apparatus as well.

A considerable period was spent in the development of an automatic optical pyrometer to be used with the transient apparatus. In its original form, the device included an internal standard light source, so that a calibration could be established once and for all. It was soon evident, however, that for viewing very

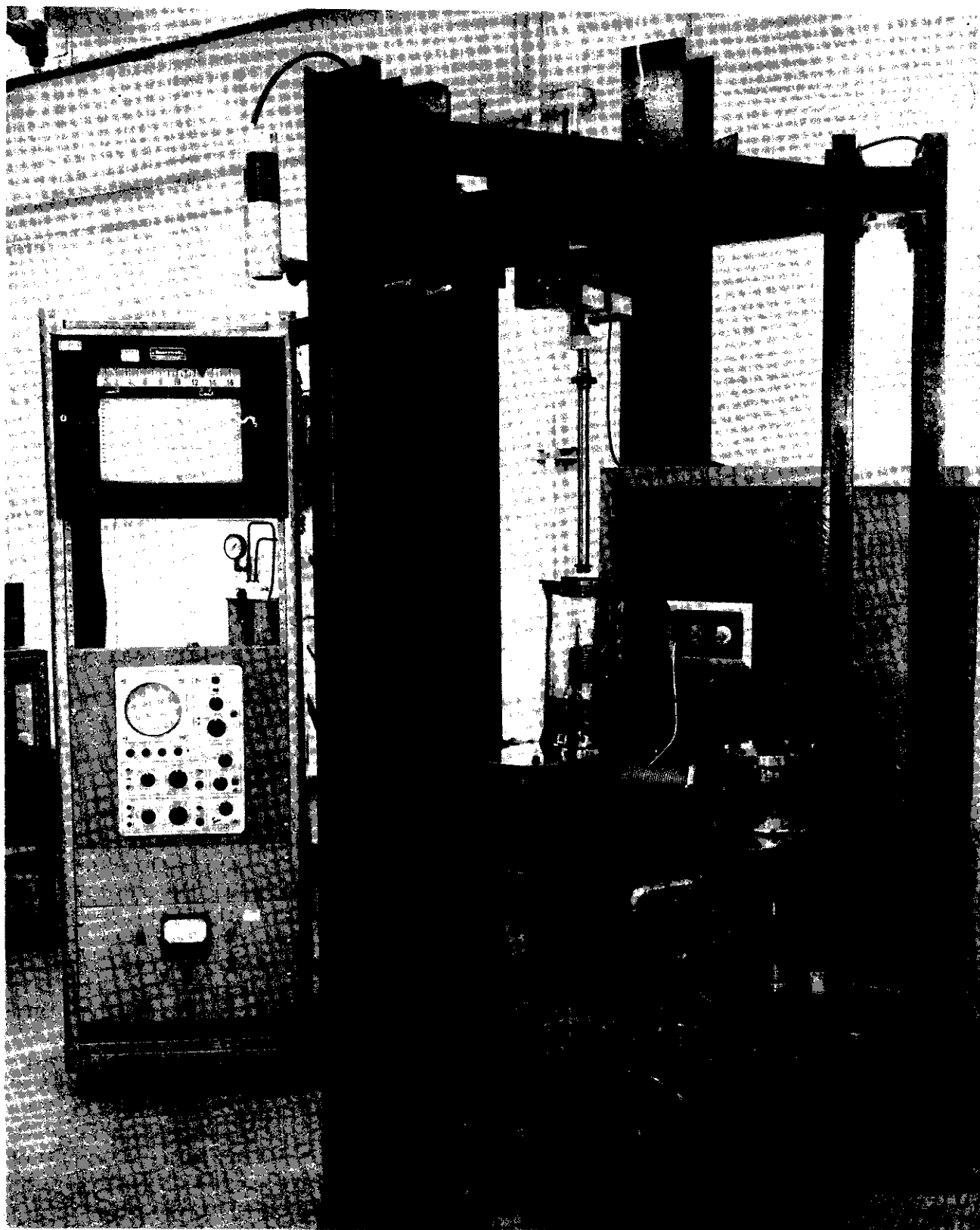


Figure 1. Transient Measurements Apparatus

Contrails

small holes at some distance from the pyrometer, the optics of the prototype were of insufficient quality to give the requisite precision and sensitivity required in the transient scheme. Moreover, the prototype signal exhibited a noise pattern arising from the complex electronics which could not be reduced to a level sufficient for the present application. It was felt that for measurements of thermal properties, accuracy in the absolute value of the temperature could be sacrificed for the purpose of achieving a more noise-free signal and at the same time maximizing sensitivity to temperature differences while maintaining rapid response. This was achieved by incorporating high-quality commercial optics with a battery-driven photomultiplier tube in a precisely machined housing. The optics include an f 2.7 Kodak Ektar Anastigmat lens of 102 mm focal length for the objective lens and an f 1.6 Somco second lens of 0.75 in. focal length. A diaphragm and cross hairs were located at the focus to insure accurate alignment. A 10x eyepiece fitted into the photomultiplier tube housing was used for the purpose of alignment. Operated as a d-c device with dry cells for the high voltage supply, the arrangement has given the lowest noise level to date. The absolute temperature is measured independently by means of a commercial optical pyrometer.

The specific heat is determined from the sample heat input rate Q_{hs} , which is related to the slopes of the time-temperature curves for the heater and sample by the relation¹

$$Q_{hs} = m_h c_h \left(\dot{T}_{h_{out}} - \dot{T}_{h_{in}} \right), \quad (2)$$

where m_h and c_h are the mass and specific heat of the heater and where the temperature derivatives,

$$\dot{T}_{h_{in}} \text{ and } \dot{T}_{h_{out}},$$

are measured with the sample in the heater and with no sample in the heater. Measurement of the slope of a curve is inherently less accurate than the accuracy with which the points on the curve itself may be determined. Electronic differentiating circuits (typically RC networks) have the advantage that they make use of approximately as much information as is contained in their time constant RC. Thus, one chooses as large a time constant as possible commensurate with the typical rate of change of the signal to be differentiated. These circuits have the disadvantage that they amplify in proportion to the frequency of variations in the signal so that low noise requirements are critically important for the present application where the total change in electronic signal occurs monotonically over a time interval of minutes. In the present arrangement, the voltage drop across a 10k resistor in series with the pyrometer photomultiplier tube is differentiated by a basic RC circuit with a time constant of 0.68 sec. The derivative signal is amplified by a Philbrick model P2 solid-state amplifier. High-frequency noise is suppressed by the amplifier and lower-frequency noise components such as 60-cycle pickup are reduced by placing a bypass capacitor in parallel with the 10k resistor. The results thus far indicate that this arrangement can measure the slopes of the

temperature-time curves with greater accuracy than graphical means. The use of curve fitting would be expected to give optimum results. However, it would be very time-consuming and will not be exploited unless other expedients are found to be impractical.

Only after incorporating the high quality optics in the pyrometer did the critical effect of the radiation shields become evident. It was observed that scattered light originating from the space between the individual shields and between the shield assembly and the sample, changed the black body character of the sight holes. This was corrected by inserting tantalum tubes of 0.001 in. wall thickness through the sight holes of the shield and placing them directly against the sample. The tubes are approximately 0.120 in. in diameter while the sample sight holes are 0.050 in. in diameter. The pyrometer may then be focused through the tubes, at the sample sight holes so that the temperature of the tube walls does not adversely affect the black body character of the sight holes. The configuration is illustrated schematically in Figure 2.

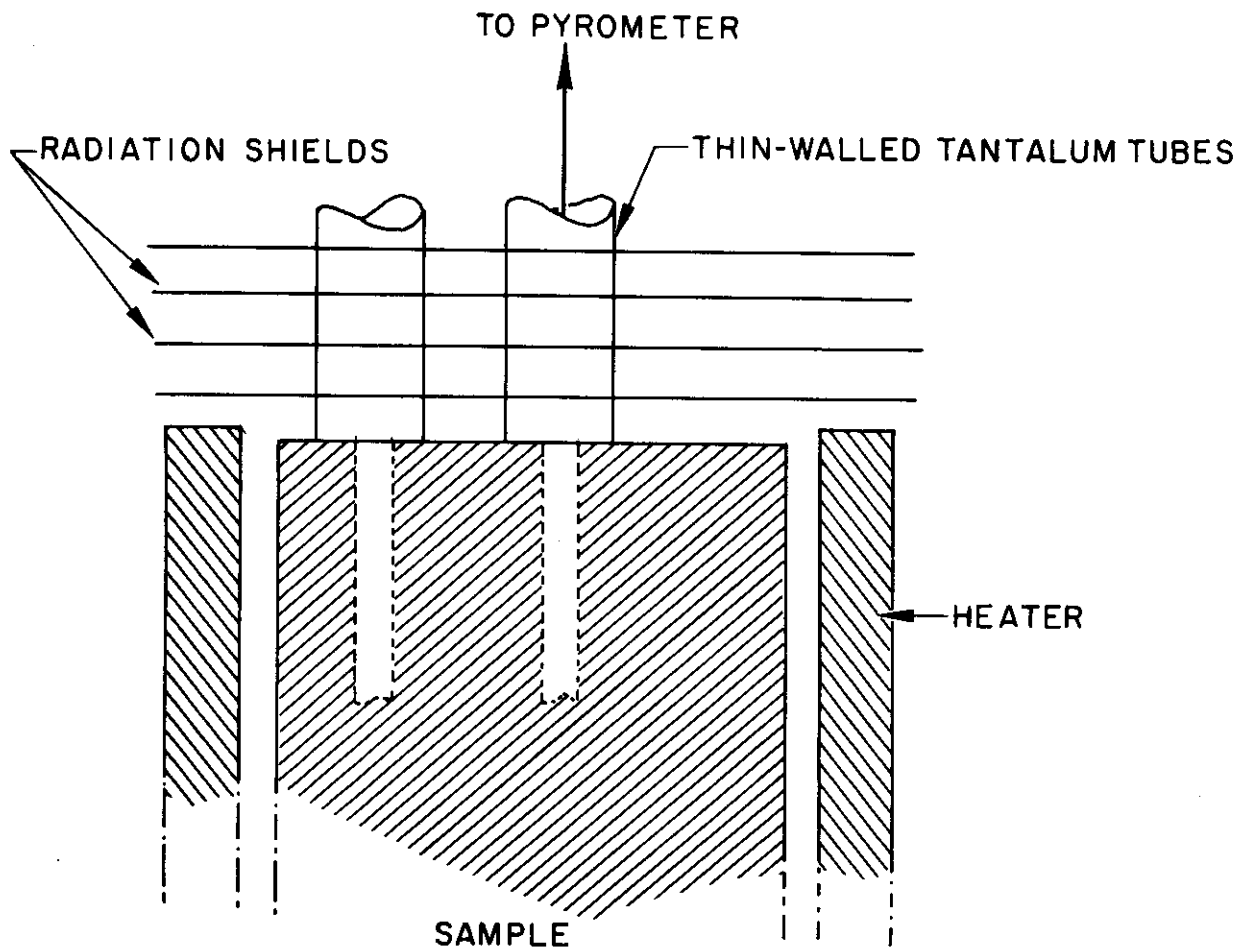


Figure 2. Schematic of Radiation Shields With Pyrometer Sight Tubes

Contrails

Because the developments reported here are quite recent, it has not been possible during this short time to complete detailed drawings to illustrate the precise geometry of the present apparatus. In a future report, when an optimum and final configuration will have been achieved, a complete description will be given.

Experimental Results

With the new pyrometer and modifications in the sample enclosure completed, trials were only recently begun on a sample of tungsten boride. This material was chosen for the initial trials because, on the basis of simple estimates, it would be expected to have smaller values of thermal diffusivity than the carbides or nitrides. The cylindrical sample was 1 in. long and 5/8 in. in diameter with 0.049-in. sight holes drilled to a depth of 1/2 in. at its longitudinal center and at a radius of 0.221 in. Its mass was 79 grams.

The data for the initial run on tungsten boride have been reduced and are plotted in Figures 3 and 4. Figure 3 shows the transient thermal response of the heater and sample when the sample is in the heater (curves 2 and 3) and of the heater when the sample is absent (curve 1).

As is expected from theoretical considerations,¹ a plateau occurs in the heater response curve when the sample is present. This may be seen on curve 2 between 80 and 120 sec on the time scale. The plateau occurs because in this region, heat is being transferred to the sample at a maximum rate. This is shown in Figure 4, where the rate of heat input to the sample has been plotted as a function of time. The points in Figure 4 have been calculated from Equation (2). It has been previously shown¹ that the accurate and simple relations

$$c_s = \frac{Q_{hs}}{m_s \dot{T}_s} \quad (3)$$

and

$$\alpha = \frac{a^2}{8\Delta t} \times (\text{correction factor}) \quad (4)$$

may be used to determine the specific heat and thermal diffusivity, provided that Q_{hs} varies no more rapidly than linearly with time. It is thus instructive and essential to plot Q_{hs} over the entire time range to determine the regions where accurate results may be expected.

In Equation (4), Δt represents the time required for the temperature of the inner sight hole in the sample ($r = 0$) to reach that of the outer hole ($r = a/\sqrt{2}$). This time is of the order of one second, so only one curve is shown in Figure 3, inasmuch as the time scale would show the two curves as essentially superimposed.

As regards Equation (4), it is easy to show that if Q_{hs} varies negligibly in the period Δt (of the order of one second), the correction factor is equal to unity, so

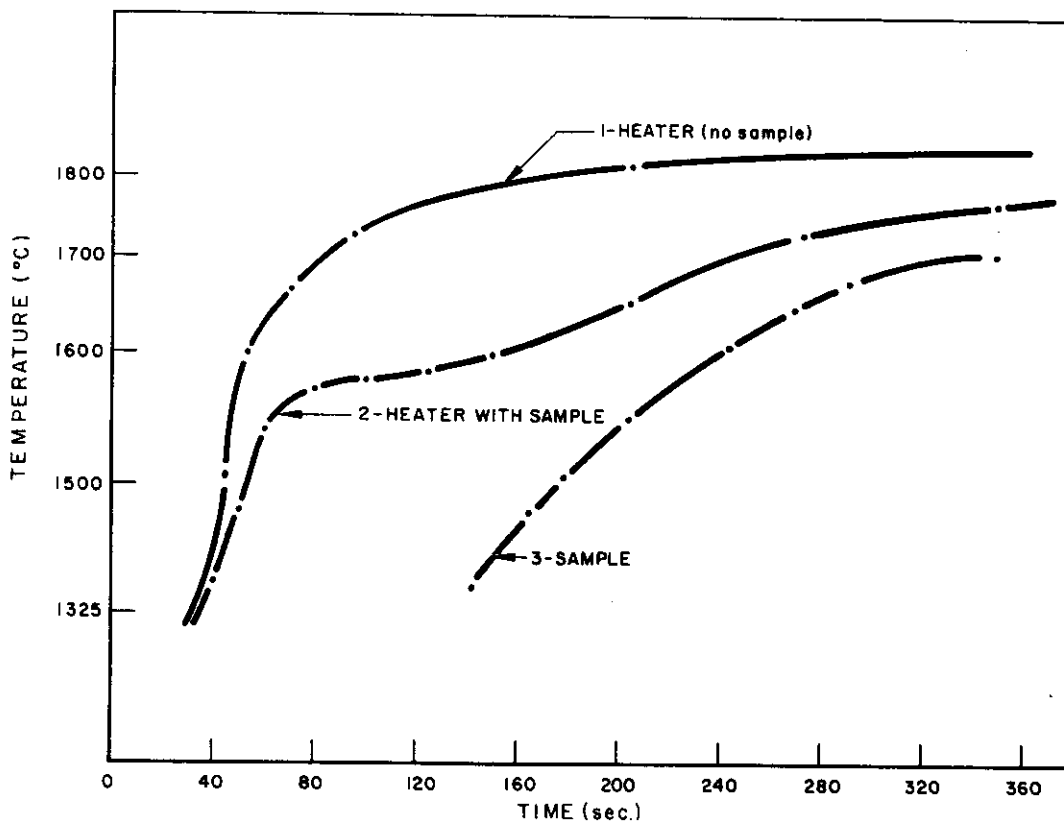


Figure 3. Thermal Response Curves for Tungsten Boride Sample

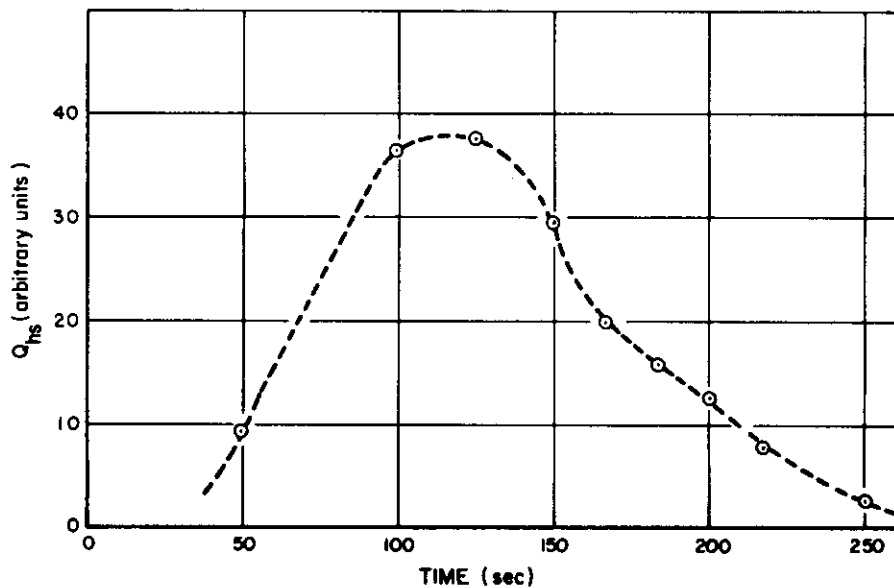


Figure 4. Time Rate of Heat Input to Tungsten Boride Sample

that Equation (4) reduces to Equation (1). Calculations indicate that this is an accurate and valid approximation for all materials whose thermal diffusivity is greater than $0.01 \text{ cm}^2/\text{sec}$. Consequently, the thermal diffusivity is expected to be given accurately by Equation (1) over the entire transient time shown in Figure 3. Using this equation the following values have been determined from the data corresponding to Figures 3 and 4.

TABLE 1
THERMAL DIFFUSIVITY OF TUNGSTEN BORIDE

T (°C)	α (cm^2/sec)
1330	0.054
1434	0.054
1534	0.058
1582	≈ 0.06
1615	≈ 0.06

On an expanded time scale such that the two curves, corresponding to the two sample sight holes, are sufficiently separated for the interval Δt to be measured, it is found that the curves have extremely shallow slopes, and this aspect is enhanced at the highest temperature, as is evident from Figure 3. Consequently, measurement of the time interval separating them becomes practically impossible at higher temperatures. For this reason the last two values of α given in Table 1 are only approximate. The possible error of measurement for the first two values of Table 1 is estimated to be less than ± 0.003 ; for the third value, about ± 0.004 . This includes errors arising from reading the graphs and arising in the measuring apparatus. It does not include errors arising from any possible departure from the theoretical thermal response of the sample due to radiation or conduction losses, though these are believed to be negligible. In fact, it previously had been experimentally established that heat conduction to the sample is negligible. Because of the difficulty in resolving the curves for the inner and outer holes at higher temperatures, one must use much higher values for the maximum heater temperature, $T_{h_{max}}$, to obtain thermal diffusivity data at higher temperatures than those given here. In fact, the use of higher values is advantageous in the transient scheme, firstly because the pyrometer sensitivity increases roughly as T^2 , and secondly because the thermal response curves become progressively steeper as $T_{h_{max}}$ increases. At present, further runs are being made at temperatures above 2000°C on tungsten boride, but have not been completed to include the data in this report. However, preliminary analysis indicates that the results are quite satisfactory. It appears that for thermal diffusivity measurements the transient apparatus is ready for operation.

The data shown on Figure 4 for the heat input rate to the sample Q_{hs} were determined graphically from the thermal response curves of Figure 3. Analysis of these data showed that such a procedure is too inaccurate to give reasonable or consistent values for the specific heat by Equation (3). Therefore, a differentiating circuit has been recently incorporated in the apparatus, and this modification appears to give results with better accuracy. As the data of all subsequent runs have

Contrails

not yet been analyzed, it remains uncertain whether accurate specific heat measurements can be made in the transient scheme without resorting to curve fitting for determination of correct slopes. Should the transient approach prove unfruitful for specific heat capacity measurements, they can be obtained efficiently at temperatures up to the melting point by the pulse technique described in the following section.

III. SPECIFIC HEAT OF BRITTLE CONDUCTORS BY THE PULSE HEATING METHOD

A pulse heating method for the measurement of the specific heat of electrical conductors was given in a previous report.¹ It was established that no difficulties were encountered in applying the method to nonbrittle metallic samples. Accuracies in the specific heats of 3% were attainable at heating rates varying from 1000° to 60,000°C/sec. However, attempts to use this method for brittle non-metals, such as the carbides, were not successful because the samples fractured during rapid heating. During the period covered by this report, the causes of sample fracture have been determined and the pulse heating method has been successfully applied to the carbides of zirconium and titanium.

The specific heat apparatus is described in detail in another report² and only a resume will be presented here. The apparatus is pictured in Figure 5. The sample, which is contained in a vacuum chamber, is connected in series with a relay, a bank of batteries, a standard resistor, and a variable resistor. When

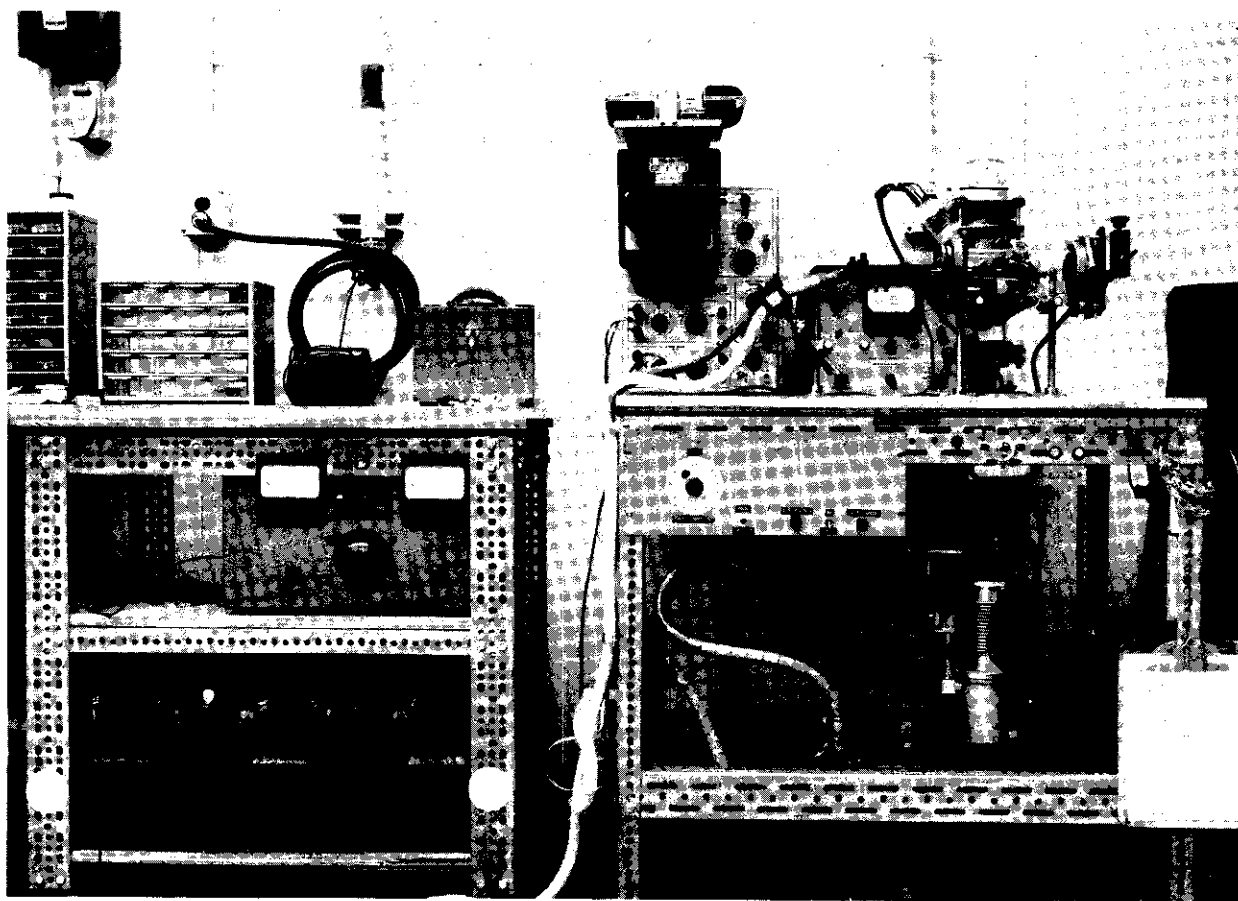


Figure 5. Specific Heat Apparatus

Contrails

the relay is closed, a surge of current flows through the circuit heating the sample. The heating rates, which may be varied from 1000° to $60,000^{\circ}\text{C}/\text{sec}$, are determined by the number of batteries used and the value of the variable resistor. The duration of the pulse is controlled by a timing circuit, and will terminate when the sample melts or at any preselected time short of melting.

The voltage drop across the central portion of the sample and the current, measured in terms of the voltage drop across the standard resistor, are recorded as a function of time by photographing the traces on a dual beam oscilloscope. At any instant the voltage and current may be determined from the photograph. A vernier-microscope is used to measure the voltage and current at definite time intervals and the specific resistance at each time interval is calculated from the relationship

$$\rho = \frac{A E}{L I} \quad , \quad (5)$$

where A is the cross-sectional area of the wire, L is the distance between voltage probes, and E and I the voltage and current, respectively. The specific heat at any temperature T is given by the expression

$$c_p = \frac{EI}{J} \frac{4}{D^2 L d} \frac{\frac{d\rho}{dT}}{\frac{d\rho}{dt}} \quad , \quad (6)$$

where c is in cal/gm, J is 4.186 watt-sec/cal, D is the diameter of the specimen, d is the density, $d\rho/dT$ is the temperature coefficient of the resistivity at temperature T , and $d\rho/dt$ is the rate of change of the resistivity at the resistance corresponding to T . This approach presupposes a knowledge of the resistance as a function of temperature, which was obtained in the present work by the standard potential drop method. An IBM 709 computer was used to smooth the measured voltages and currents and to calculate the resistivity, its derivative and thus the specific heat.

To investigate the reasons for sample fracture, it was felt that studies on test materials of varying brittleness would be informative. Uranium silicide was chosen as the test material because its brittleness is controlled by the percentage of silicon present. Therefore attempts to heat the material by the pulse technique could be tried on less brittle samples and as techniques and apparatus were improved, the test could be conducted on samples of increased brittleness. Furthermore, uranium silicide was readily available at reasonable cost. While developing the techniques, the data obtained are found to be of general interest and are incorporated as a significant portion of this report.

Uranium silicide samples were prepared by arc melting weighed amounts of uranium and silicon and then casting the melt. The cast material was analyzed chemically to determine the loss of silicon due to vaporization so that the results would be appropriately corrected. Sample histories are given in Table 2. Three

compositions were used, 3.8% silicon (U_3Si), 5.9% silicon ($U_3Si + U_3Si_2$) and 7.3% silicon (U_3Si_2).

TABLE 2
SAMPLE HISTORIES OF URANIUM SILICIDE

Number	% U	% Si	Density (gm/cm ³)	Composition
533	96.2	3.8	14.5	U_3Si^*
535	96.2	3.8	14.3	U_3Si^*
539	94.1	5.9	12.9	$U_3Si_2^\dagger + U_3Si^*$
7-806	92.7	7.3	12.1	U_3Si_2

* U_3Si tetragonal

† U_3Si_2 body-centered tetragonal

Studies indicated that sample failures were caused by three mechanisms: (a) stresses arising from thermal expansion, (b) stresses arising from torque caused by the surge of current, and (c) arcing from the current contacts to the sample. The use of flexible leads allowed for thermal expansion but increased the torque problem. Consequently, it was necessary to employ rigidly mounted pistons which permitted the sample to expand and contract freely in one direction while maintaining a current path suitable for carrying the several thousand amperes required to heat a specimen. The use of these pistons eliminated thermal stress and torque problems. However, arcing at the sample-to-piston contacts proved to be a severe problem which could not be overcome by various clamping techniques. Arcing occurred at or near the end of the clamps, especially if tight tolerances between the sample and contact were not maintained. Although precise machining apparently would overcome this difficulty, this is very hard to accomplish on brittle materials; therefore alternate approaches were sought. The method which proved most satisfactory involved nickel-plating the ends of the specimen and soft-soldering the sample to the holders. The solder melts during pulse heating to high temperatures, but this causes no difficulty except that the walls of the vacuum chamber are plated with a metallic film. A photograph of a mounted sample and an exploded view of a piston is shown in Figure 6. With this arrangement, it was possible to heat uranium silicide samples repeatedly by the pulse technique. Runs were also made successfully on the carbides of zirconium and titanium. An example of one of these electronically machined specimens is shown in Figure 7. These runs have indicated a necessary change in the sample holders. In particular, the initial alignment of the pistons has been found to be critical as well as time-consuming. A dove-tail track is being constructed to overcome this problem. Alternate methods of fixing the sample to the holder are being studied; for example, the use of nickel foil inserts is being investigated. This, however, is not a critical refinement. The applicability of the pulse heating technique to brittle conductors may be regarded as an established development.

To determine specific heat capacity by the pulse heating technique, as presently conceived, it is necessary that the temperature derivative of the electrical resistivity be known. This is indicated by Equation (6). Initial attempts to measure

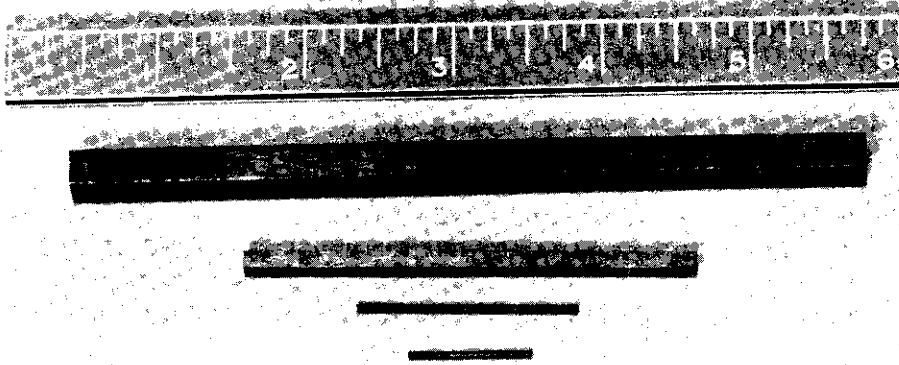


Figure 6. Closeup of Mounted Sample

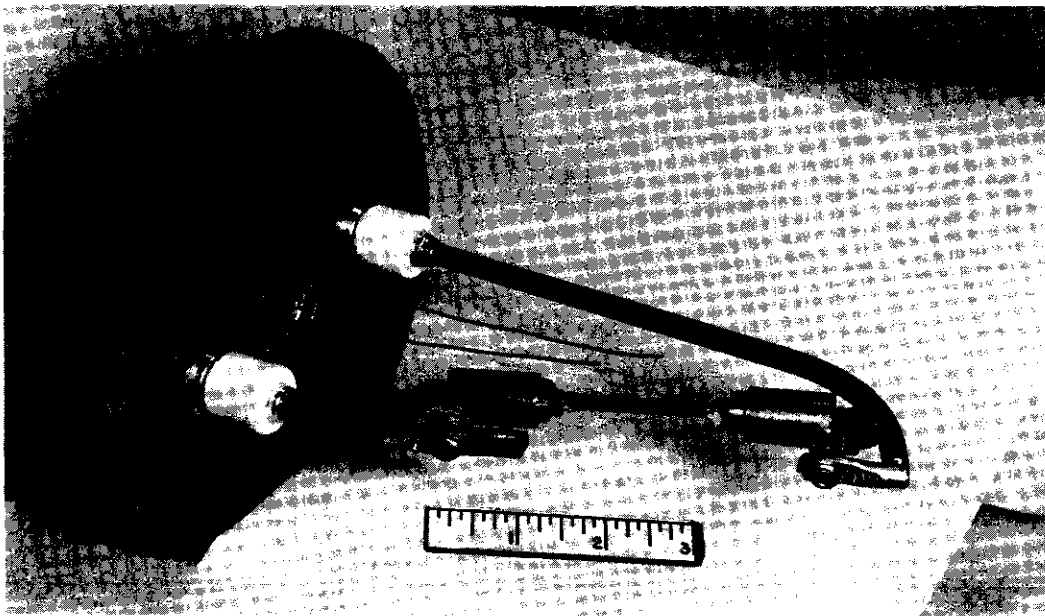


Figure 7. Electrically Machined Specimens for Specific Heat Measurements

the electrical resistivity of uranium silicide were unsuccessful because of a marked tendency for the resistivity to change from heating cycle to heating cycle. After several cycles of raising the sample temperature to 600°C and then a 24-hr anneal at 800°C, the resistivities of the 3.8% and 5.9% samples were found to attain constant values. After similar treatment, however, the 7.3% material continued to vary in its resistivity. The final values for the 3.8% and 5.9% samples, and the last measurements on the 7.3% sample are shown in Figure 8. These results point up the fact that for certain refractory materials the thermal properties may depend markedly on the sample history, method of preparation, and impurity content. When this is the case, reliable and physically meaningful measurements may be expected to result only after extensive annealing at high temperatures or else when other methods are used to ensure homogeneity and thermal stability of the bulk material. In the present case, even with arc-cast material of prescribed stoichiometry, it is evident that the virgin material may have unstable physical properties.

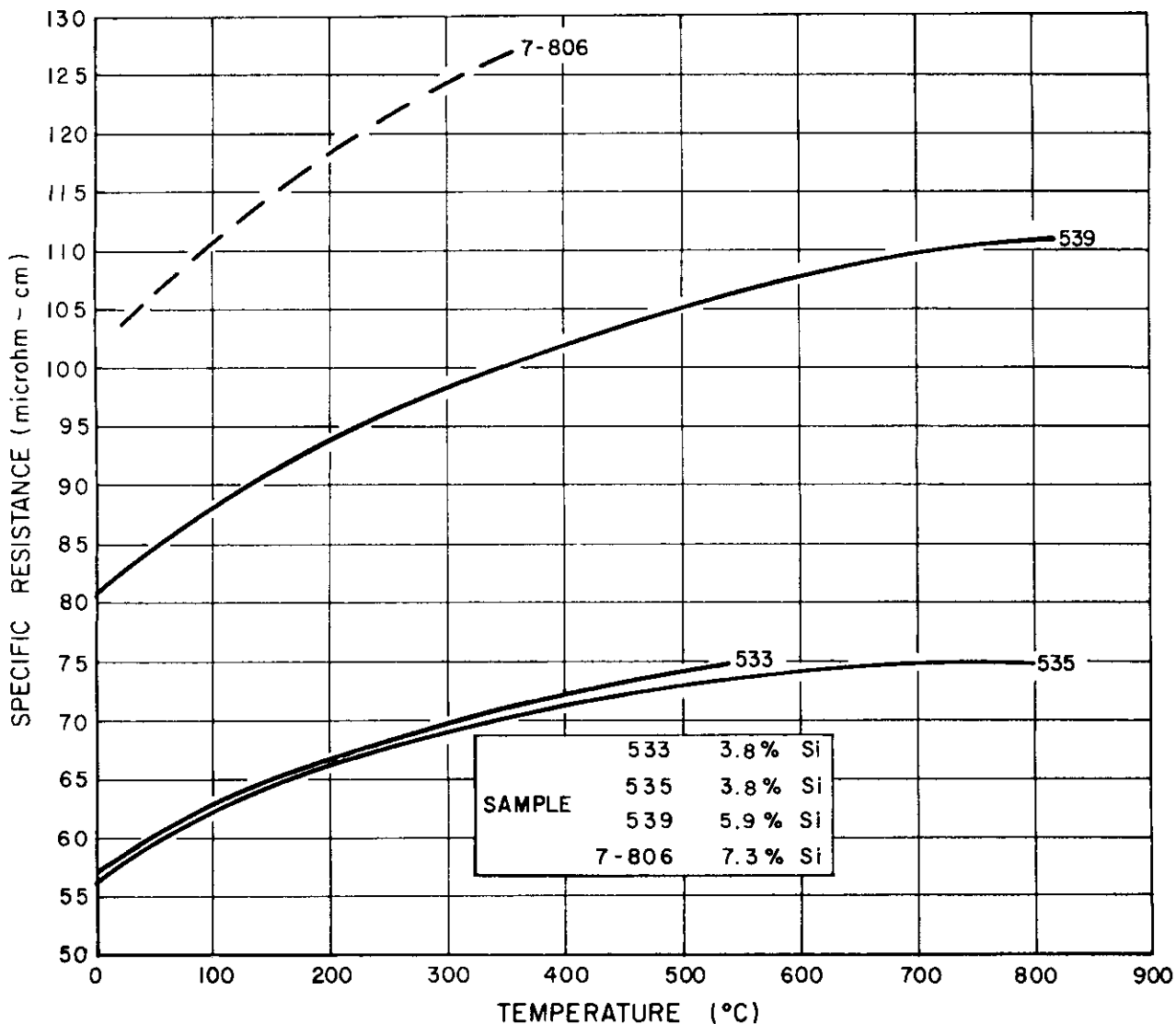


Figure 8. Resistivity of Uranium Silicide

From Figure 8, it may be seen that the resistivity of uranium silicide increases with increasing silicon content. This is to be expected from the DuLong-Petit law. Figure 8 shows also that the resistivity of uranium silicide tends to become constant at higher temperatures. For this reason the specific heat of the 3.8% material could not be determined accurately above 500°C.

The data from three runs on sample 533* and one run on sample 535 (both 3.8% Si) were analyzed and plotted. The results are shown in Figure 9. The specific heats of both specimens increased linearly with temperature and are given by

$$c_p = 3.16 \times 10^{-6}T + 0.0412 \quad \text{cal/gm-}^\circ\text{C from } 50^\circ \text{ to } 430^\circ\text{C}, \quad (7)$$

where T is in °C. A total of 118 data points were obtained on samples 533 and 535. These data all fell within 5% of the curves shown in Figure 9. The data from two runs on sample 539 are shown on Figure 9 also. The specific heat of this specimen was found to increase linearly with temperature and can be expressed as

$$c_p = 16.1 \times 10^{-6}T + 0.0455 \quad \text{cal/cm-}^\circ\text{C from } 50^\circ \text{ to } 715^\circ\text{C}. \quad (8)$$

A total of 70 data points were obtained and all were within 6% of the curve shown in Figure 9.

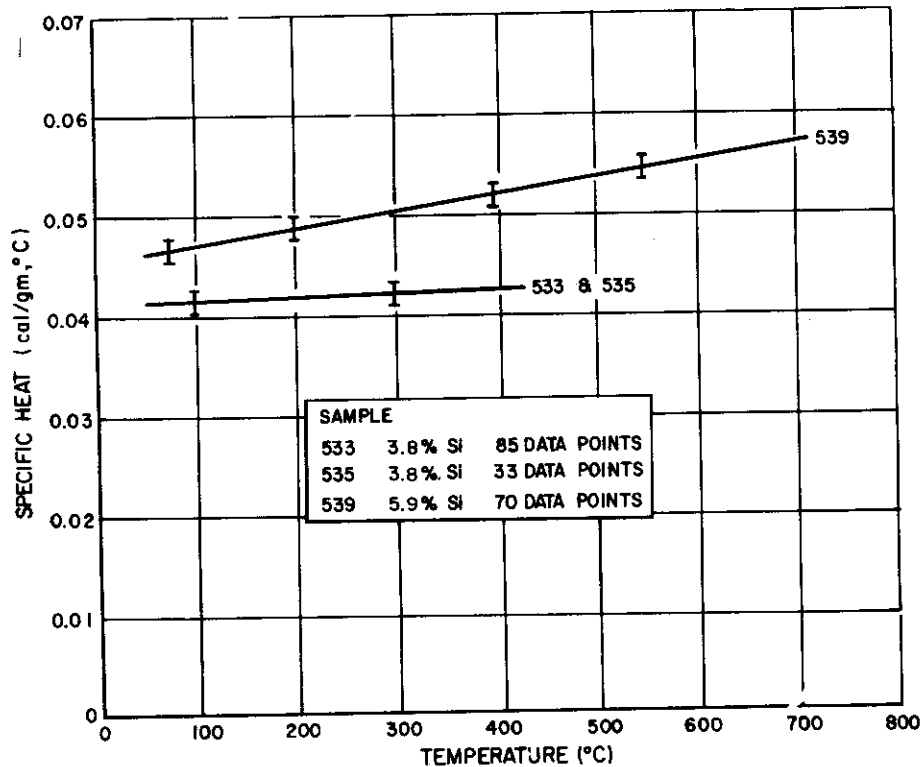


Figure 9. Specific Heat Capacity of Uranium Silicide

*These are identification numbers assigned by the Materials Development Department at Atomics International.

The specific heat of uranium silicide increases with increasing silicon content as expected from the DuLong-Petit law. Values of the specific heat of various uranium silicides calculated from this law are presented in Table 3. The 3.8% material corresponds to U_3Si , the 7.3% material corresponds to U_3Si_2 , and the 5.9% material represents a two-phase system of U_3Si_2 and $U Si_3$. Based on the phase diagram for the uranium-silicon system, the specific heats of these materials should show no anomalies up to $930^\circ C$, which is beyond the range of the present measurements. The maximum temperature used in the present measurements was limited by the thermal expansion allowed by present sample holders. Although only minor modifications were necessary to extend the range, the major objective of the present work was the development of specific heat measurement techniques, and therefore no attempts were made to obtain resistivity data at high temperatures.

TABLE 3
CALCULATED SPECIFIC HEATS OF URANIUM SILICIDES

Compound	Formula Weight	Number of Atoms	Specific Heats*
U	238	1	0.0269
U_3Si	742	4	0.0359
U_3Si_2	770	5	0.0416
U Si	266	2	0.0482
U Si_2	294	3	0.0653

*Calculated from $c_s = \frac{6.4 \times \text{number of atoms}}{\text{Formula weight}}$

The chief difficulties in making a specific heat capacity determination of uranium silicide by the present approach are connected with its resistivity measurements. As stated previously, the resistivity of the 7.3% material did not stabilize, whereas the change in resistivity of the 3.8% material with temperature approached zero at higher temperatures (i. e., above $500^\circ C$). Consequently, the specific heat of the 7.3% material could not be measured at any temperature and the specific heat of the 3.8% samples could not be measured above $500^\circ C$.

During the initial work on metals, a method of directly measuring the rate of change of temperature was studied and found to be feasible.² When this quantity is measured directly, the requirements that the resistivity as a function of temperature be known, that the resistivity measurements be reproducible, and that the change in resistivity with temperature is not zero, are no longer applicable. It is expected that the use of this method, which is based on the sample acting as the thermocouple junction, may allow the measurement of the specific heat in those cases where it cannot be determined by the present procedure.

IV. THERMAL CONDUCTIVITY BY STEADY-STATE METHOD

The thermal conductivity of titanium carbide has been measured from 500° to 2100°C using the steady-state radial heat flow furnace previously described.³ A photograph of the furnace is shown in Figure 10. This furnace has been used to measure the thermal conductivity of graphite, molybdenum, tantalum⁴ and BeO.⁵ The procedures used in the present work were very similar to those used previously and will not be discussed here. Past experience as well as present measurements on standards materials have shown that accuracies of 10% or better may be expected.

The Carborundum Corporation supplied us with the titanium carbide samples prepared by a hot-pressing method. For thermal conductivity measurements in the steady-state apparatus, the material was electrically machined into the form of cylinders 2.0 in. OD, 0.50 in. ID, and 3.0 in. in length.

The densities were between 94 and 95% of theoretical and chemical analysis showed less than 0.3% metallic impurities present. X-ray examinations indicated that the samples were composed of a single phase.

About five separate runs were made on each of three samples. The results are shown in Figure 11, along with those of Vasilos and Kingery,⁶ whose data are the only published measurements at high temperatures. The lack of agreement between the two results is readily apparent, although it is interesting to note that the room temperature values (obtained by extrapolation) do agree. The cube sample used by Vasilos and Kingery was nearly identical in density and in metallic impurity content to those used in the present work.

In an attempt to explain the present results, the electrical resistivities of the titanium carbide samples were measured from 0° to 800°C. The values of resistivity were found to increase from about 60 to 110 micro-ohm-cm over this temperature range. The resistivity values are plotted in Figure 12. The room temperature value of resistivity measured in the present work is in good agreement with that reported for the cube sample.⁶ With these resistivity values, the contribution to the thermal conductivity due to electrons was calculated using the Wiedemann-Franz law, and the results are shown as the curve k_e in Figure 11. The total conductivity (k_t) can be expressed as

$$k_t = k_e + k_p, \quad (9)$$

where k_p is the contribution due to phonons. This relationship implies that the electron and phonon contributions are independent. This approximation is expected to be reasonably valid at the temperatures in question. If so, the total conductivity should lie above the curve k_e , as is observed in the present work. However, the total conductivity falls below k_e for the cube sample of Vasilos and Kingery unless the electrical resistivity above room temperature (not given by Vasilos and Kingery) increases very rapidly.

A different way of presenting the above argument is to calculate the Lorenz number, L , as a function of temperature. For good metals above room temperature, L is independent of temperature and theoretically equal to 5.36×10^{-9} cal-ohm/sec-°C². For alloys, poor metals, and non-metals, the measured value of

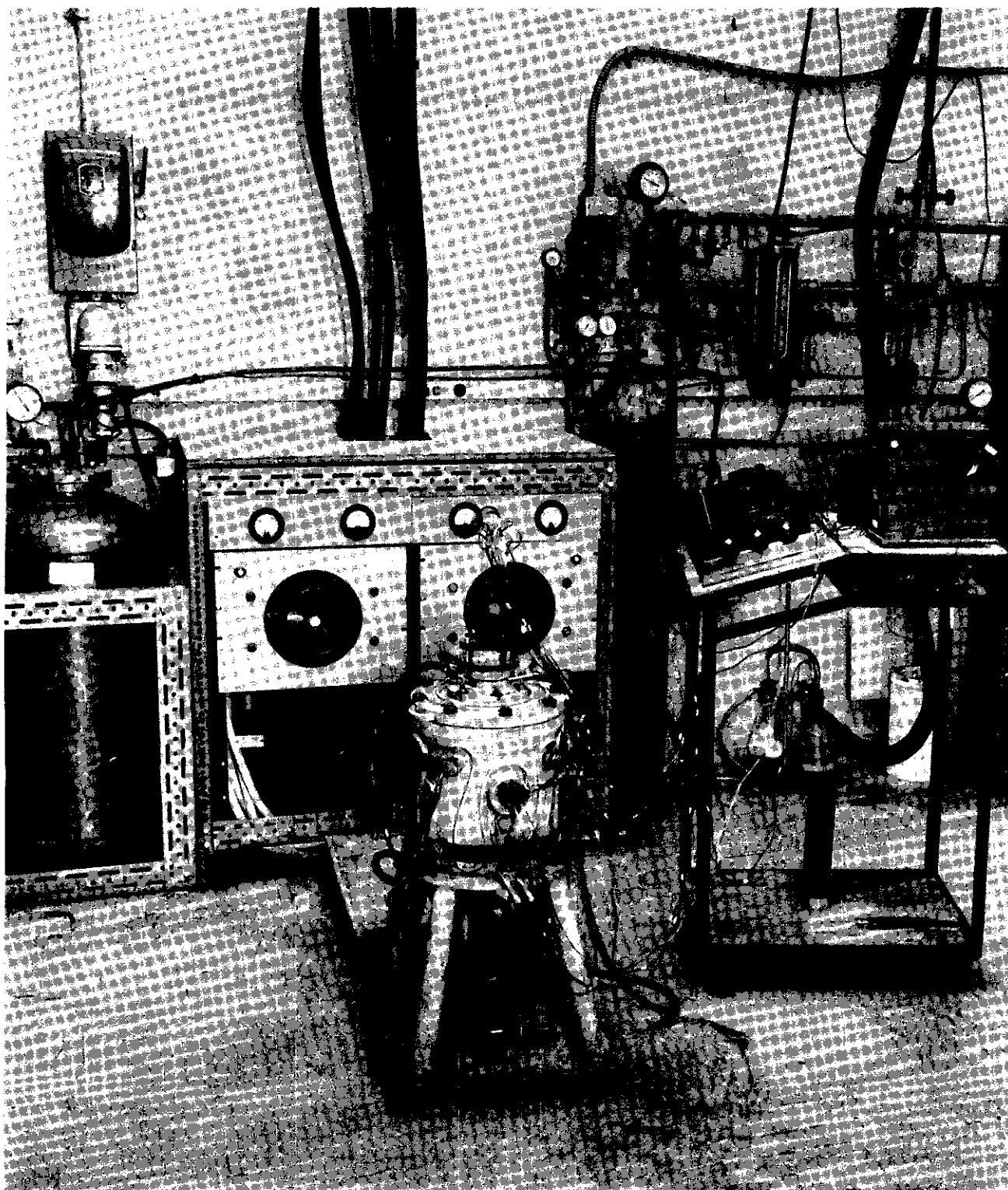


Figure 10. Steady-State Thermal Conductivity Furnace

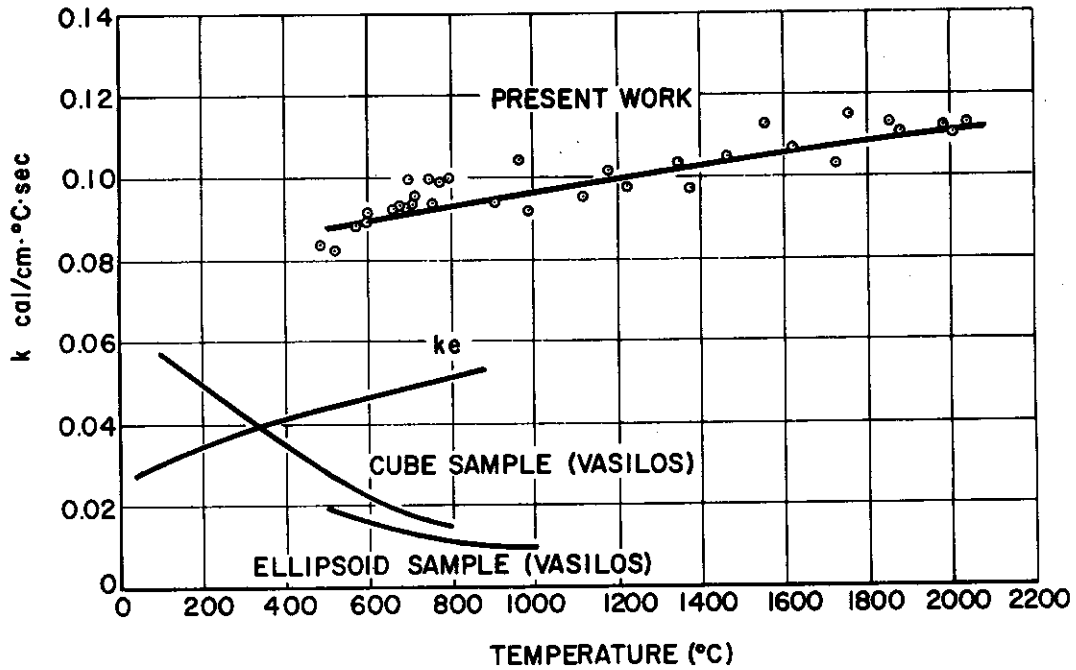


Figure 11. Thermal Conductivity of Titanium Carbide

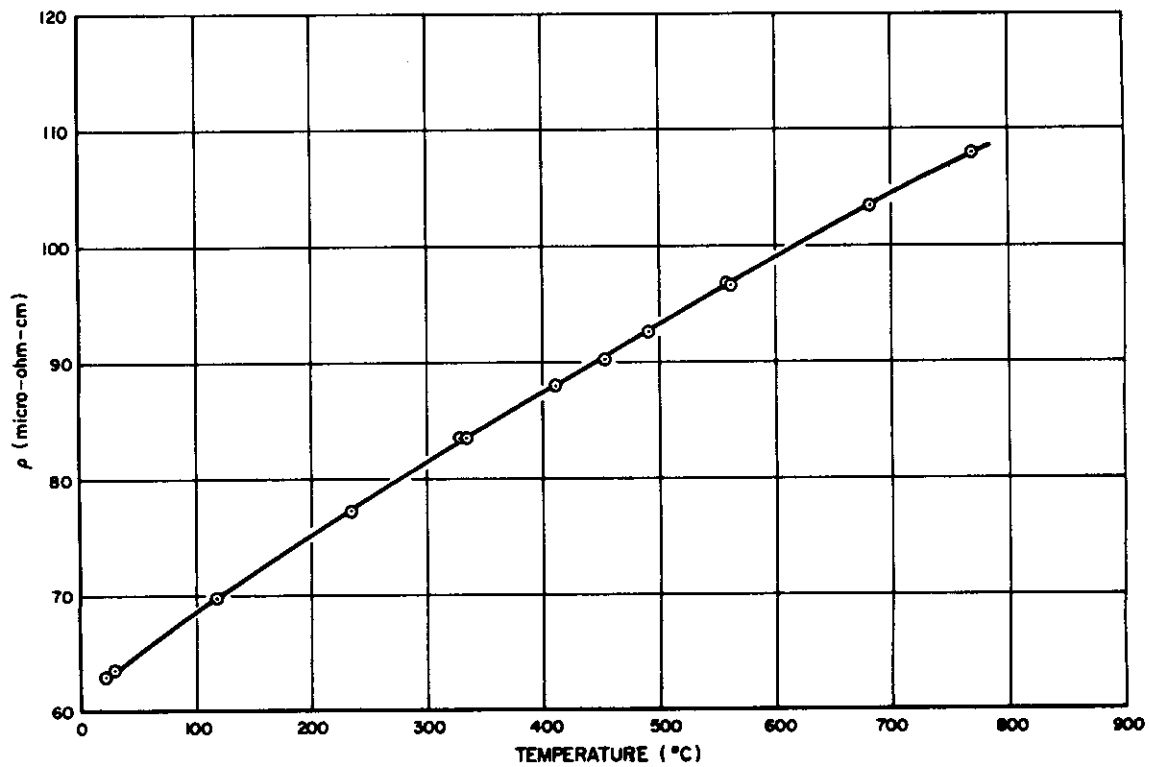


Figure 12. Electrical Resistivity of Titanium Carbide

L is greater than the theoretical value for metallic conductors, but approaches that value as the temperature is increased. For example, for graphite at room temperature, L is 200 times the theoretical number, but approaches the latter number at higher temperatures. Alloys are a less extreme example. L is often a factor of two above the theoretical value at room temperature and asymptotically approaches the theoretical value as the temperature is increased.

The values of L for titanium carbide computed in the present work decrease from 1.49×10^{-8} at 0°C to 9.45×10^{-9} at 800°C , or a decrease of from 2.8 to 1.8 times the theoretical value. The value of L calculated for the cube sample falls below the theoretical value above 350°C unless the electrical resistivity increases extremely rapidly. An increase from 60 to 450 micro-ohm-cm in the temperature range 0° to 800°C is required to keep L above the theoretical value. This is a marked departure from the measured values shown on Figure 12.

The only other published thermal conductivity measurements for titanium carbide are $0.041 \text{ cal/cm-sec-}^\circ\text{C}$ at room temperature reported by Schwarzkopf and Kieffer⁷ and $0.0263 \text{ cal/cm-sec-}^\circ\text{C}$ from 20° to 100°C reported by Glazer and Ivanick⁸ for a sample of pure dense titanium carbide. These results are far below the values reported either by Vasilos and Kingery or the present work. Despite the discrepancy with literature values, the total conductivity results of the present work shown in Figure 11 are believed accurate within 10% and are consistent with the resistivity data. However, due to the increasing interest in the use of carbides for high-temperature applications, there is an urgent need for further investigations of the thermal properties of these materials. For example, k_p , obtained by subtracting k_e from k_t , apparently does not follow the $1/T$ relationship. The departure from the $1/T$ law indicates that further studies are required for an understanding of the processes involved.

Electrical and thermal conductivity measurements were also made on samples of zirconium carbide, and the results are in qualitative agreement with that observed for titanium carbide. The electrical resistivity was measured by the a-c bridge method previously used for metallic samples² and by the standard potentiometric method. The results are plotted in Figure 13. The thermal conductivity was found to increase from about $0.075 \text{ cal/cm-sec-}^\circ\text{C}$ at 600°C to $0.080 \text{ cal/cm-sec-}^\circ\text{C}$ at 1100°C . These are preliminary results based on one specimen only. Further measurements are planned.

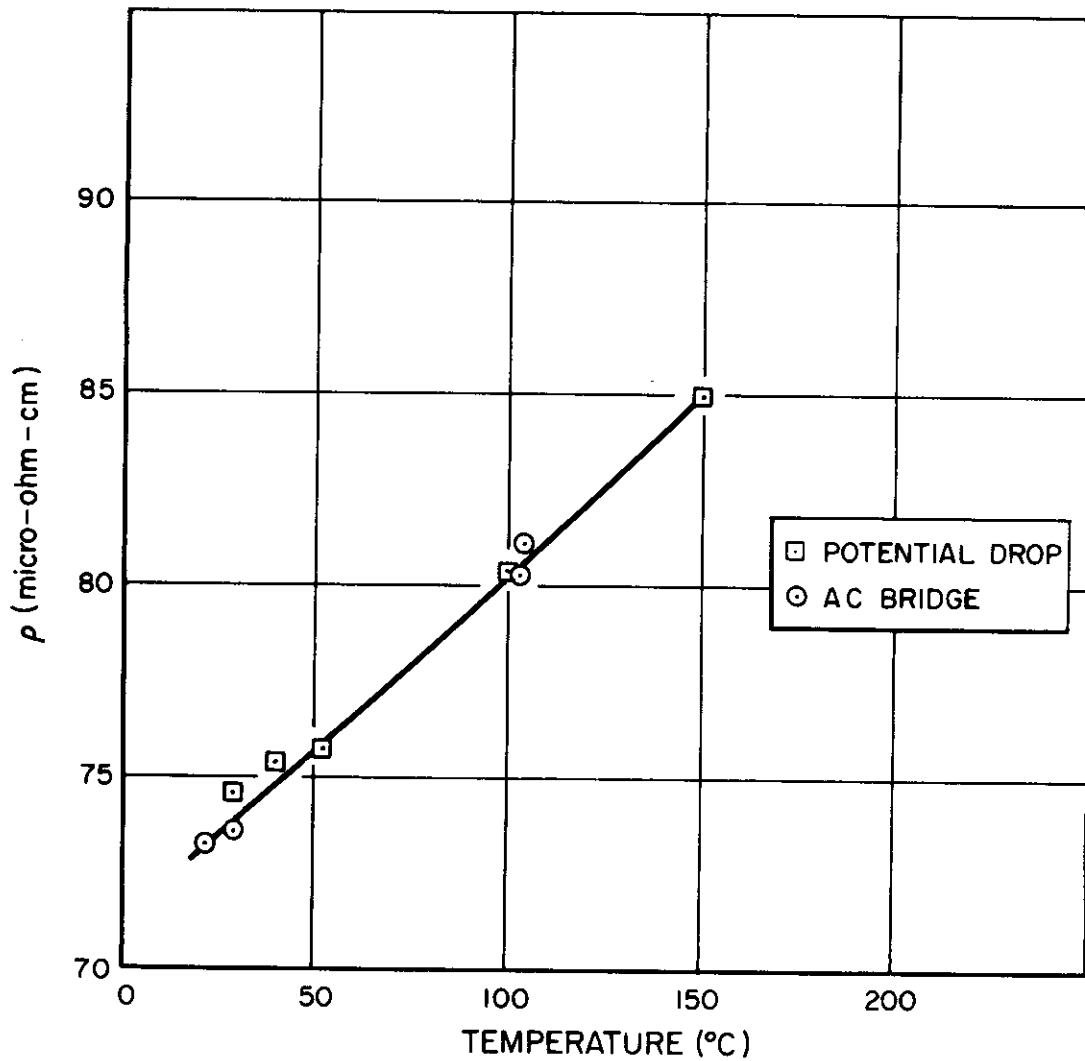


Figure 13. Electrical Resistivity of Zirconium Carbide

V. BIBLIOGRAPHY

1. G.W. Lehman, WADD Tech. Report 60-581, Thermal Properties of Refractory Materials, July 1960
2. R.E. Taylor and R.A. Finch, The Specific Heats and Resistivities of Molybdenum, Tantalum, and Rhenium to Very High Temperatures, NAA-SR 6034 (1961)
3. N.S. Rasor and J.D. McClelland, Rev. Sci. Inst., 31, 595 (1960)
4. N.S. Rasor and J.D. McClelland, Int. J. Phys. Chem. Solids, 15, 17 (1960)
5. R.E. Taylor, NAA Tech. Report, NAA-SR-4905, Thermal Conductivity and Thermal Expansion of BeO at Elevated Temperatures, July 1960
6. T. Vasilos and W.D. Kingery, J. Am. Ceram. Soc. 37, 409 (1954)
7. P. Schwarzkopf and R. Kieffer, Refractory Hard Metals, the Macmillan Co., N.Y. (1953)
8. F.W. Glazer and W. Ivanick, J. of Metals 4, 378 (1952)